



Effect of glass compression plate on EBT-XD film dosimetry for pretreatment quality assurance of stereotactic body radiotherapy

Sathiya Raj , Nithya Shree , K M Ganesh

Department of Radiation Physics, Kidwai Memorial Institute of Oncology, Bangalore, India

ABSTRACT

Background: EBT-XD film specially designed for high dose verifications such as stereotactic treatments. The dose response of the film can be affected by several factors, the curly nature of the film being one of them. In this study this curly nature of the film was investigated for stereotactic body radiotherapy (SBRT) plan verifications.

Materials and methods: For this study, 18 SBRT (11 prostate, 3 spines, and 4 lungs) cases were enrolled. For all the cases, VMAT plans were created in the Monaco treatment planning system and plan was delivered in Elekta Versa HD linear accelerator and delivered fluence was captured by EBT-XD films. All films were scanned with and without a compression plate. All the films were analyzed using the single-channel film method using the red channel.

Results: A significant difference in the gamma passing rates (GPR) for the films scanned with and without the compression plate was observed. The maximum percentage differences in GPR between using and not using a compression plate were 12.7% for 1% 1 mm, 8.1% for 2% 2 mm, 7.5% for 3% 2 mm, and 5% for 3% 3mm criteria. Similarly, the mean %difference in GPR was 5.8% for 1% 1 mm, 2.4% for 2% 2 mm, 1.6% for 3% 2 mm and 0.96% for 3% 3 mm criteria.

Conclusion: The results suggest that placing a compression plate over the film during scanning provided a great advantage in achieving a more accurate gamma passing rate irrespective of gamma criteria.

Key words: film dosimetry; curve fitting; gamma analysis

Rep Pract Oncol Radiother 2024;29(3):357-361

Introduction

Despite the availability of many commercial array-based detectors in the market, EBT films continue to play a crucial role in radiotherapy due to their higher spatial resolution, energy dependency in megavoltage beams, dose rate independency, and tissue equivalency [1-4]. However, they come with certain uncertainties in dosimetry, such as inter and intra-film variations, errors in film position-

ing during scanning, waiting time after irradiation, and the inability to provide 3D dose information [5-7]. Moreover, the curved nature of the film can cause errors in dose analysis. Palmer et al. identified this issue and proposed a simple solution using a glass compression plate during the scanning process. Their study found that smaller film samples are more susceptible to errors if scanned without a compression plate [8]. However, there is a lack of literature on the impact of the compression plate

Address for correspondence: Sathiya Raj, Assistant Professor, Department of Radiation Physics, Kidwai Memorial Institute of Oncology, Bangalore, India; e-mail: sathiarajmedphy@gmail.com

This article is available in open access under Creative Common Attribution-Non-Commercial-No Derivatives 4.0 International (CC BY-NC-ND 4.0) license, allowing to download articles and share them with others as long as they credit the authors and the publisher, but without permission to change them in any way or use them commercially

in stereotactic body radiation therapy (SBRT)/stereotactic therapy (SRT)/stereotactic radiosurgery (SRS) cases, especially where the target size is smaller compared to conventional fractionation targets. Additionally, there is no available information on the effect of the compression plate on different gamma criteria. As the target sizes are smaller in SBRT, the film requirement is also reduced. Therefore, to quantify the effect of the compression plate, we aimed to conduct a study for SBRT cases using different gamma criteria. The study aimed to investigate how the compression plate affects dose analysis accuracy in SBRT cases with smaller target sizes and different gamma criteria. This research will fill the existing gap in literature and potentially provide insights into the efficacy of the compression plate for improved dose analysis accuracy in SBRT cases.

Materials and methods

Linac calibration

Prior to irradiating the films, linac reference dosimetry was carried out using a Farmer-type ion chamber in a water phantom sized $30 \times 30 \times 30 \text{ cm}^3$. The beam quality used for calibration of the film was 6 MV photon beam. The calibration coefficient of the chamber can be traceable to secondary standard dosimetry laboratory (BARC-India). The source-to-surface distance (SSD) was set to 100 cm, and the field size was adjusted to $10 \times 10 \text{ cm}^2$. The chamber was positioned at the depth of 10 cm (calibration depth) from the water surface. Meter readings for each polarity were repeated six times. All necessary correction factors, as per TRS 398 guidelines, were duly applied [9].

Monitor Unit (MU) Calculation for film calibration

A slab phantom (PMMA-material), measuring 40 cm in length (l), 40 cm in breadth (b), and 15 cm in height (h), was scanned using a Philips Big Bore CT scanner. The scanning settings were configured at 120 kVp, 200 mAs, with a slice thickness of 3 mm. The resulting scanned phantom images were exported to the Monaco Treatment Planning System (TPS) version 5.51.10. From the TPS, the monitor units (MUs) necessary to deliver known doses were obtained for dose levels ranging from 0.5 to 30 Gy (at 0.5, 2, 5, 8, 12, 16, 20, 25, and 30 Gy). The dose

was calculated at a depth of 5 cm from the surface of the phantom. Collapsed cone convolution algorithm was used to calculate the MUs in the TPS.

Film exposure

A small strip of film, approximately $4 \times 4.5 \text{ cm}^2$, was cut into 10 pieces for calibration purposes. Film exposure was carried out immediately following the linac reference dosimetry. The film irradiation was conducted using the Elekta Infinity linac employing a 6 MV X-ray beam energy. The SSD was set to 100 cm, and the field size was adjusted to $10 \times 10 \text{ cm}^2$. These films were positioned at the depth of 5 cm within the slab phantom. As the MUs were obtained from the same setup via the TPS, there was no necessity to place the films at a water-equivalent depth in the slab phantom. To monitor any unexpected output fluctuations in the linac, a Farmer-type ion chamber was positioned at the bottom of the phantom. This chamber was placed well below the film's depth (10 cm) to prevent any disturbances that might impact the film dose.

Treatment planning and delivery

In the current study, a total of 18 SBRT cases were enrolled, comprising 11 prostate cases, 3 spine cases, and 4 lung cases. For all cases, VMAT plans were performed using the Monaco treatment planning system version 5.51.10. The plans were executed with the following parameters: a) Grid size set to 0.2 cm, b) Statistical uncertainty set to 1% per calculation, c) 180 control points per arc, and d) Minimum segment width set to 0.5 cm. Full arcs were utilized for all cases, except lung cases, for which partial arcs were employed. Once the plans were completed, they were exported to the Mosaic record and verification system for scheduling. Clinical plans were re-calculated on the solid water block (PMMA) phantom for subsequent measurement with the film. The plans were subsequently delivered using the Elekta Versa HD linear accelerator.

Film scanning protocol

Before initiating the scanning process, the vertical maximum air gap between film and scanner was measured four times, and these values were duly recorded. The exposed films were scanned in red channel using an EPSON Expression 12000XL flatbed scanner. The scanning procedure was executed using the film-scan applica-

tion provided by PTW. All calibration films were scanned after a 24-hour post-irradiation period. Given the known curvature tendencies of EBT-XD films, which could potentially reduce contact with the scanner, a 3 mm thick pure glass compression plate was utilized to ensure optimal contact with the scanner bed. The scanner settings were configured to the transmission mode with a 48-bit TIFF image (each channel containing 16 bits), and the scan resolution was set to 75 dots per inch. To avoid lateral scanner artefacts, all films were positioned at the central axis of the scanner. Additionally, colour corrections were deactivated. As part of the scanning process, seven dummy scans were initially performed without a film to allow for warm-up. Following this, seven scans were conducted with the films, with the exclusion of the first two scans to derive the Pixel values (PVs) for each exposed and unexposed film.

The above scanning procedure was repeated by removing the glass compression plate from the scanner to get one more calibration curve, this will be used while scanning the clinical plan's films without glass compression plate.

Calibration curve generation

PTW FilmCal software version 2.4. was used to extract pixel intensities. The optical density was defined by the following equation:

$$\text{net OD} = \log_{10} \left(\frac{I_{\text{unexp}}}{I_{\text{exp}}} \right)$$

Here, I_{unexp} and I_{exp} are PVs of unexposed and exposed films. There were two calibration curves generated: one was a film scanned without a compression plate, the other was a film scanned with a compression plate. To analyse the impact of a glass compression plate, all exposed films (SBRT plans) were scanned with and without a compression plate and an appropriate calibration curve was used. During scanning the position of the films was kept the same to avoid any positional error.

Gamma analysis

Once the SBRT plan exposed films scanned, they were exported to PTW verisoft application for gamma analysis. The gamma analysis was performed for 1%1mm, 2%2mm, 3%2mm and 3%3mm for global normalization. The low dose threshold was kept as 10%.

Results

Uncertainty budget

Table 1 shows the uncertainty components in the current study. The linac output measurements were repeated 6 times and the variation in the output was stated as one of the uncertainty components (Tab. 1). For scanner uniformity, a film was scanned in different places (around central axis-within 7cm in all directions) of the scanner and standard deviation (SD) of PVs was obtained. Inter film uniformity was obtained by scanning the same film multiple times and for each film PVs were obtained in a different location of the film to get the SD of PVs. Films were scanned with different orientation (0°, 45° 90°, 180° and 270°), the PVs were obtained in each position to know the position error in terms of SD in the PVs for each position. The fitting function of PTW verisoft was unknown. This fitting uncertainty was excluded from the current uncertainty budget, as this may underestimate the total uncertainty.

Comparison of dose response curves

Figure 1 shows the calibration curve of a film with and without a compression plate. To assess the reliability of curve fitting, the predicted dose from the fitting model was compared with the delivered dose. The fitting model for the dose response given by PTW verisoft exhibited an average percentage difference of 0.6% for dose range from 2 to 30 Gy. The gap between the film and the film scanner bed was measured using a ruler for 18 films, with four repeated measurements. The maximum separation between the film and the scanner bed was 1.48 mm, with an average of 1.24 mm.

Gamma analysis

The maximum percentage differences in gamma passing rates (GPR) between using and not us-

Table 1. Measurement uncertainty (%) in the dose prediction

Uncertainty Component	Uncertainty
Linac output	0.5
Scanner uniformity	0.42
Positional error	0.25
Interfilm uniformity	0.43
Total uncertainty	0.8
Expanded uncertainty (K=2)	1.6

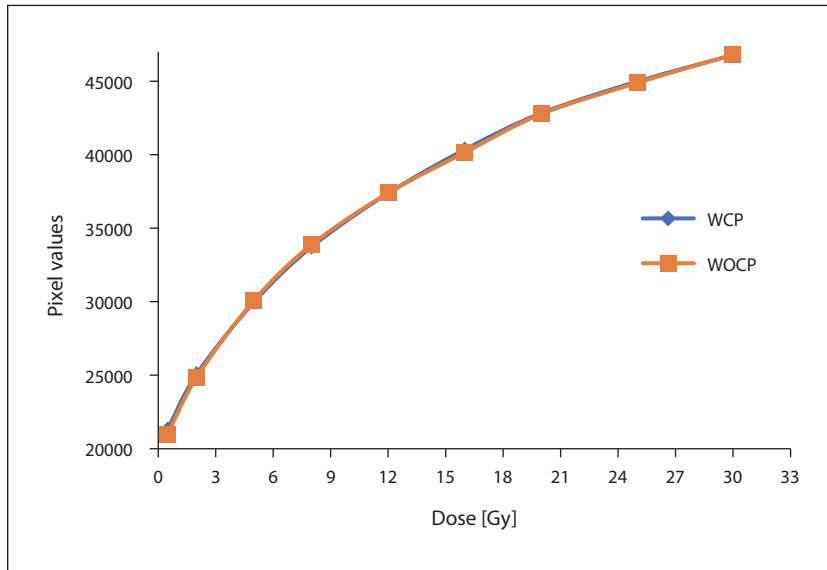


Figure 1. Dose response curve of film scanned from flatbed scanner. WCP — with compression plate; WOCP — without compression plate

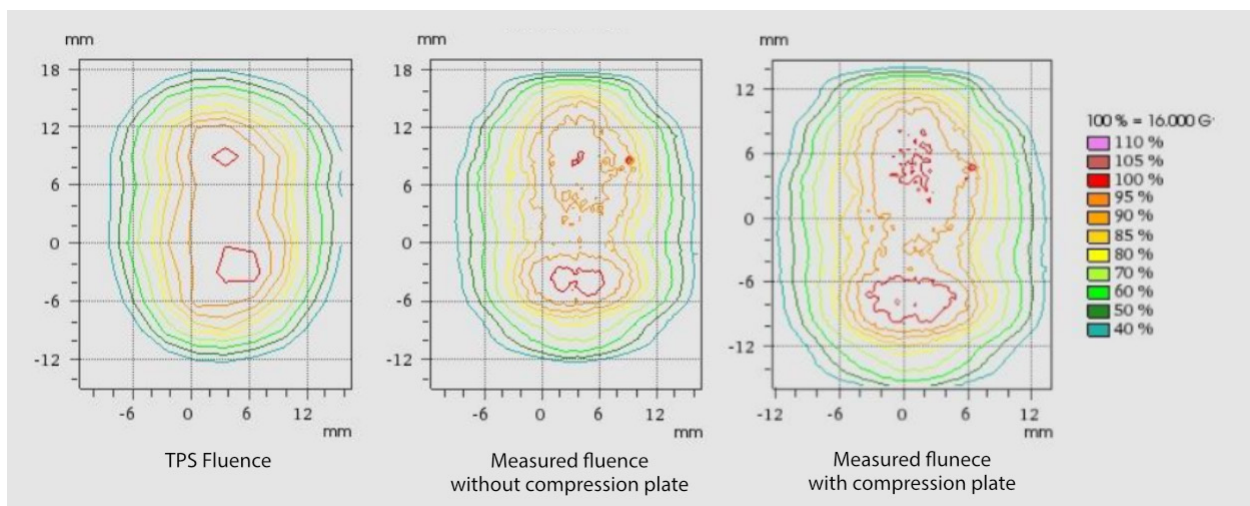


Figure 2. Gamma analysis of one of the clinical stereotactic body radiation therapy (SBRT) plan without [96% gamma passing rates (GPR)] and with compression plate (97.4% GPR) in 2%2mm gamma criteria

ing a compression plate were 12.7% for 1%1mm, 8.1% for 2%2mm, 7.5% for 3%2mm, and 5% for 3%3mm criteria. The mean %difference in GPR was 5.8% for 1%1mm, 2.4% for 2%2mm, 1.6% for 3%2mm and 0.96% for 3%3mm criteria. The GPR data with and without the compression plate was subjected to statistical analysis. Student’s t-test was conducted to determine the statistical significance of these differences. Statistical significance was observed for the following gamma criteria: 1%1mm ($p = 0.0015$), 2%2mm ($p = 0.0015$), 3%2mm

($p = 0.0027$), and 3%3mm ($p = 0.026$). Figure 2 depicts the GPR comparison for one of the cases.

Discussion

Regarding the usefulness of a compression plate in film dosimetry, Palmer et al. indicated that the natural curvature of the film during scanning, causing a maximum height 1 to 2 mm above the scan plane, may lead to a 1% to 4% dose error and considerably reduce gamma passing rates

[8]. For smaller targets, smaller films are preferable to avoid wastage, but they tend to cause more dose errors. This was investigated in this study for SBRT cases. A significant difference in GPR for the films scanned with and without a compression plate was observed, indicating the necessity of a compression plate for film scanning. In SBRT cases, setting tighter gamma criteria (1%1mm and 2%2mm) showed significant differences in GPR for films scanned with and without a compression plate. If a compression plate was not placed on the film it tended to form a concave shape on the scanner plate. Due to this concavity, the light passing through the film may experience different path length and differential attenuation across the film. This differential attenuation of the light severely affects the film response and error in the OD or PVs. This error is significantly reflected in the GPR. Despite all gamma criteria having P-values less than 0.05, it was notably lower for tighter criteria such as 1%1mm and 2%2mm. Therefore, it's evident that a compression plate is essential when using tighter gamma criteria, limiting the dose error within 2.5% for 2%2mm and 5.8% for 1%1mm in SBRT cases. The drawback of the study is the exclusion of analysing the film in a triple-channel mode, which could reduce the uncertainty due to various active layer thicknesses of the film, surface perturbations, and lateral scanner effect [10]. More accurate results could be anticipated by employing a compression plate with a triple-channel dosimetry.

Conclusion

The use of a compression plate to manage film displacement due to the film's curling nature above the scanner plate was investigated for SBRT cases. The compression plate was found beneficial, regardless of the gamma criteria used for SBRT cases. It was evident that without a compression plate, errors may increase up to 12.7%, especially for tighter gamma criteria. The film's curling nature must be considered during scanning to minimize potential

errors in dose comparison between the treatment planning system and measured doses.

Conflict of interests

Authors declare no conflict of interests

Funding

None declared.

Reference

1. Mirza J, Park H, Park SY, et al. Use of radiochromic film as a high-spatial resolution dosimeter by Raman spectroscopy. *Med Phys*. 2016; 43(8Part1): 4520–4528, doi: [10.1118/1.4955119](https://doi.org/10.1118/1.4955119), indexed in Pubmed: [27487869](https://pubmed.ncbi.nlm.nih.gov/27487869/).
2. Chełmiński K, Bulski W, Georg D, et al. Energy dependence of radiochromic dosimetry films for use in radiotherapy verification. *Rep Pract Oncol Radiother*. 2010; 15(2): 40–46, doi: [10.1016/j.rpor.2010.02.003](https://doi.org/10.1016/j.rpor.2010.02.003), indexed in Pubmed: [3863243](https://pubmed.ncbi.nlm.nih.gov/3863243/).
3. Karsch L, Beyreuther E, Burris-Mog T, et al. Dose rate dependence for different dosimeters and detectors: TLD, OSL, EBT films, and diamond detectors. *Med Phys*. 2012; 39(5): 2447–2455, doi: [10.1118/1.3700400](https://doi.org/10.1118/1.3700400), indexed in Pubmed: [22559615](https://pubmed.ncbi.nlm.nih.gov/22559615/).
4. Devic S, Tomic N, Lewis D. Reference radiochromic film dosimetry: Review of technical aspects. *Phys Med*. 2016; 32(4): 541–556, doi: [10.1016/j.ejmp.2016.02.008](https://doi.org/10.1016/j.ejmp.2016.02.008).
5. Marroquin E, González JH, López MC, et al. Evaluation of the uncertainty in an EBT3 film dosimetry system utilizing net optical density. *J Appl Clin Med Phys*. 2016; 17(5): 466–481, doi: [10.1120/jacmp.v17i5.6262](https://doi.org/10.1120/jacmp.v17i5.6262), indexed in Pubmed: [27685125](https://pubmed.ncbi.nlm.nih.gov/27685125/).
6. Khaferllari I, Kim J, Liyanage R, et al. Clinical utility of Gafchromic film in an MRI-guided linear accelerator. *Radiat Oncol*. 2021; 16(1), doi: [10.1186/s13014-021-01844-z](https://doi.org/10.1186/s13014-021-01844-z), indexed in Pubmed: [8236160](https://pubmed.ncbi.nlm.nih.gov/8236160/).
7. Méndez I, Rovira-Escutia J, Casar B. A protocol for accurate radiochromic film dosimetry using Radiochromic.com. *Radiol Oncol*. 2021; 55(3): 369–378, doi: [10.2478/raon-2021-0034](https://doi.org/10.2478/raon-2021-0034), indexed in Pubmed: [8366735](https://pubmed.ncbi.nlm.nih.gov/8366735/).
8. Palmer A, Bradley D, Nisbet A. Evaluation and mitigation of potential errors in radiochromic film dosimetry due to film curvature at scanning. *J Appl Clin Med Phys*. 2015; 16(2): 425–431, doi: [10.1120/jacmp.v16i2.5141](https://doi.org/10.1120/jacmp.v16i2.5141), indexed in Pubmed: [26103181](https://pubmed.ncbi.nlm.nih.gov/26103181/).
9. International Atomic Energy Agency. Absorbed Dose Determination in External Beam Radiotherapy. *Tech Rep Ser*. 2024; 398(Rev. 1), doi: [10.61092/iaea.ve7q-y94k](https://doi.org/10.61092/iaea.ve7q-y94k).
10. Palmer A, Bradley D, Nisbet A. Evaluation and implementation of triple-channel radiochromic film dosimetry in brachytherapy. *J Appl Clin Med Phys*. 2014; 15(4): 280–296, doi: [10.1120/jacmp.v15i4.4854](https://doi.org/10.1120/jacmp.v15i4.4854), indexed in Pubmed: [25207417](https://pubmed.ncbi.nlm.nih.gov/25207417/).